Electronic Supplementary Material (ESI) for Journal of Materials Chemistry A.

Supplementary Information

Synergistic Effect of Cation Mixing in Mesoporous $Bi_xFe_{1-x}VO_4$ Heterojunction Photoanodes for Solar Water Splitting

Mengyuan Zhang, Khue Huu Pham, Yanan Fang, Ying Fan Tay, Fatwa F. Abdi* and Lydia H. Wong*

Supplementary notes

1. Definitions and calculations of charge transfer efficiency and charge separation efficiency

We define the following efficiency terms: (i) J_{abs} is the total absorbed photons expressed as the photocurrent density, (ii) η_{sep}, the charge separation efficiency, is the number of electron-hole pairs separated in the bulk to reach the surface per absorbed photon , and (iii) η_{trans}, the charge transfer efficiency (also called catalytic efficiency or surface efficiency), is the portion of the photogenerated holes that successfully takes part in the water oxidation process after reaching the material surface.

From UV-vis absorption spectra, the calculated J_{abs} for all compositions are shown in **Figure S6**. J_{abs} can be calculated by multiplying absorption by the AM1.5 solar photon flux and integrating the product for wavelengths between 350 nm and the absorption edge of each films (350 nm is the lower integration limit due to FTO substrate absorbs below 350 nm). The equation is as follows.

$$J_{abs} = \int_{350}^{\lambda_{edge}} (A\% \times \phi_{AM1.5}(\lambda) \times e) d_{\lambda}$$

where λ_{edge} is the absorption edge wavelength for the calculated film, A% is the absorption at the specific wavelength λ, $\Phi_{\mathrm{AM1.5}}(\lambda)$ is the solar photon flux at the wavelength λ, e is the electron charge, λ is the wavelength.

Assuming that no surface recombination and facile charge transfer occur in the presence of hole scavenger (H_2O_2 in this case), both η_{sep} and η_{trans} can be calculated as follows:[1, 2]

$$\eta_{\mathrm{sep}} = J_{H_2O_2}/J_{\mathrm{abs}} \qquad \text{(S1)}$$

$$\eta_{\mathrm{trans}} = J_{H_2O}/J_{\mathrm{H_2O_2}} \qquad \text{(S2)}$$

2. Electrochemical active surface area (ECSA) measurements.

Electrochemical active surface area measurement was performed in 0.1 M KPi (pH = 7) by cyclic voltammetry at different scan rate, i.e., 20 mV/s, 50 mV/s, 100 mV/s, 150 mV/s. 200 mV/s, and 300 mV/s. For each scan rate, the capacitive current from double layer charging can be taken from cyclic voltammograms in a potential range where no Faradaic processes are observed. The capacitive current is then plotted as a function of the scan rate, and the slope of the fitting curve is a function of the electrochemically active surface area (**Figure S16a**). Comparing the slopes of different films therefore allows the comparison of the relative surface area. Detailed explanation can be seen in other reports.[3, 4]

Table S1. Comparison of photocurrent of samples fabricated by spray pyrolysis and electrospinning at 1.5 V vs. RHE in 0.1M KPi (pH=7)

Photoanode	Photocurrent at 1.5 V vs. RHE in 0.1M KPi (pH=7) (mA cm^{-2})	
	Spray pyrolysis 450 °C for 2h	Electrospinning 550 °C for 3h
$FeVO_4$	0.01	0.07
Bi50	0.34	1.18
$BiVO_4$	0.31	0.11

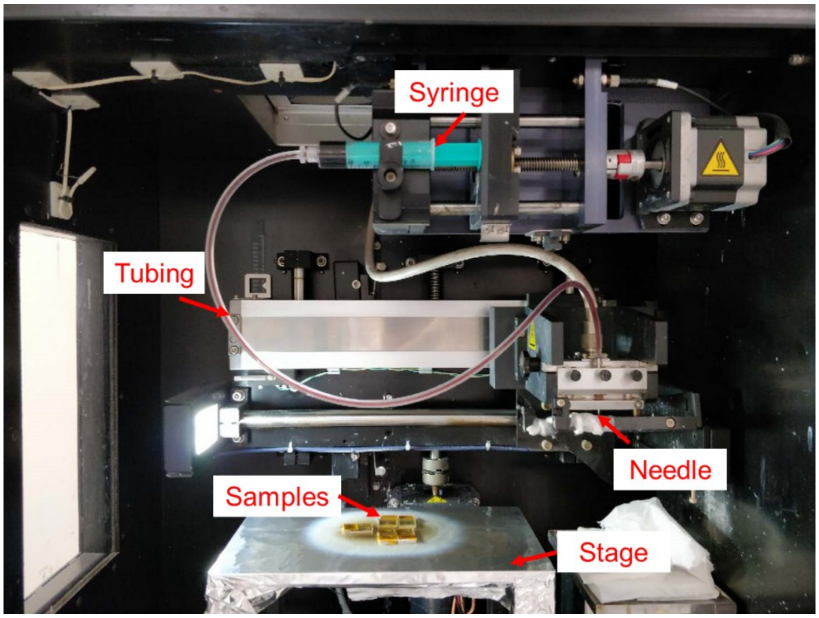

Scheme S1 Illustration of the electrospinning setup in idle condition. During deposition, the needle moves along the slide to the center position.

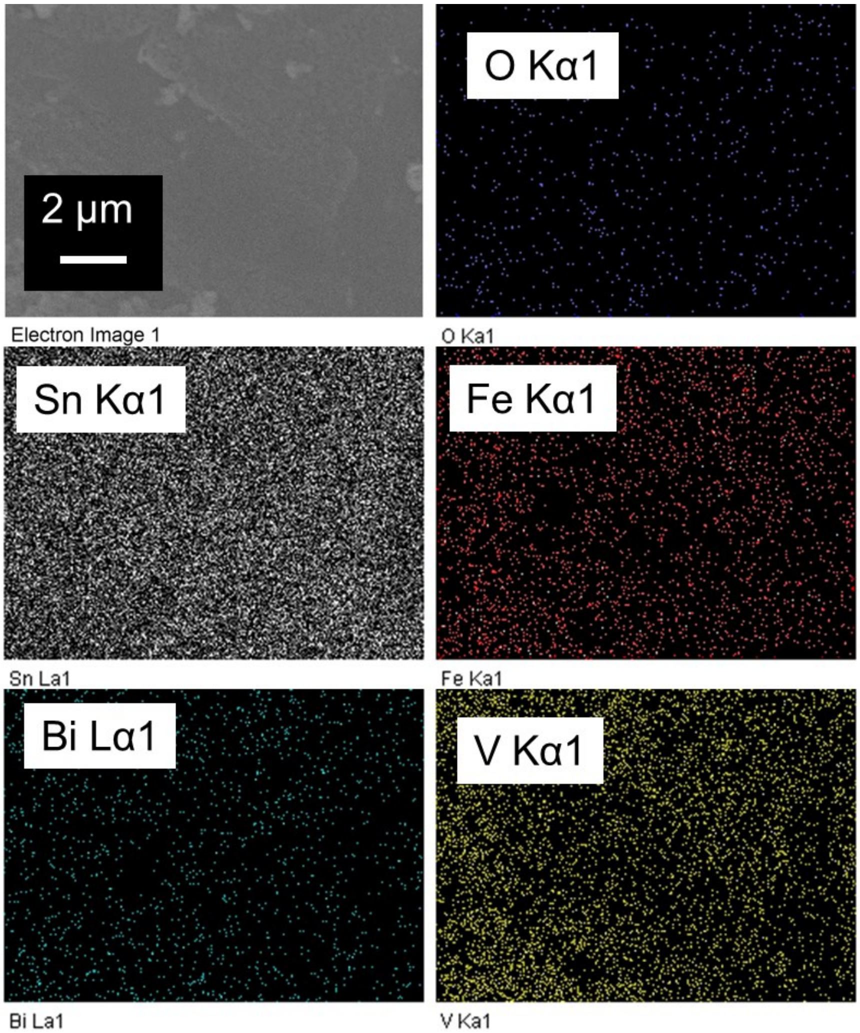

Figure S1 EDX elemental mapping of Bi50 film.

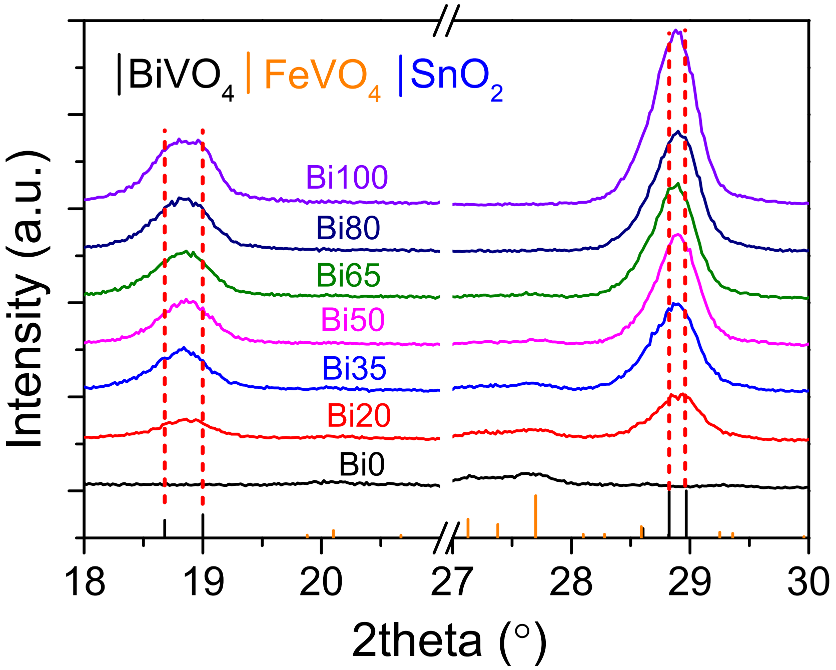

Figure S2 XRD peak position of two strong BiVO$_4$ peaks for Bi0 to Bi100, showing no obvious peak shift.

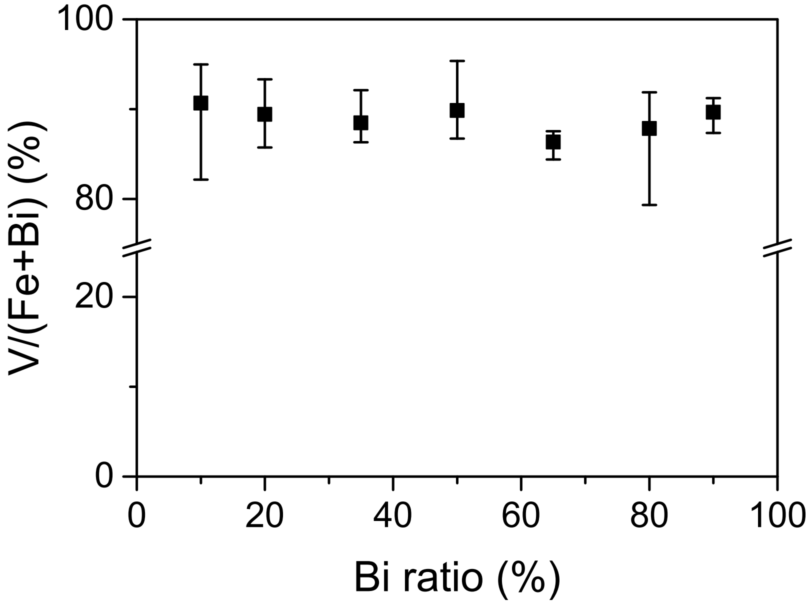

Figure S3 V/(Bi+Fe) ratio determined from EDX for films with varying Bi ratio. Atomic ratio V/(Fe+Bi) in the precursor equals to 100% in all films.

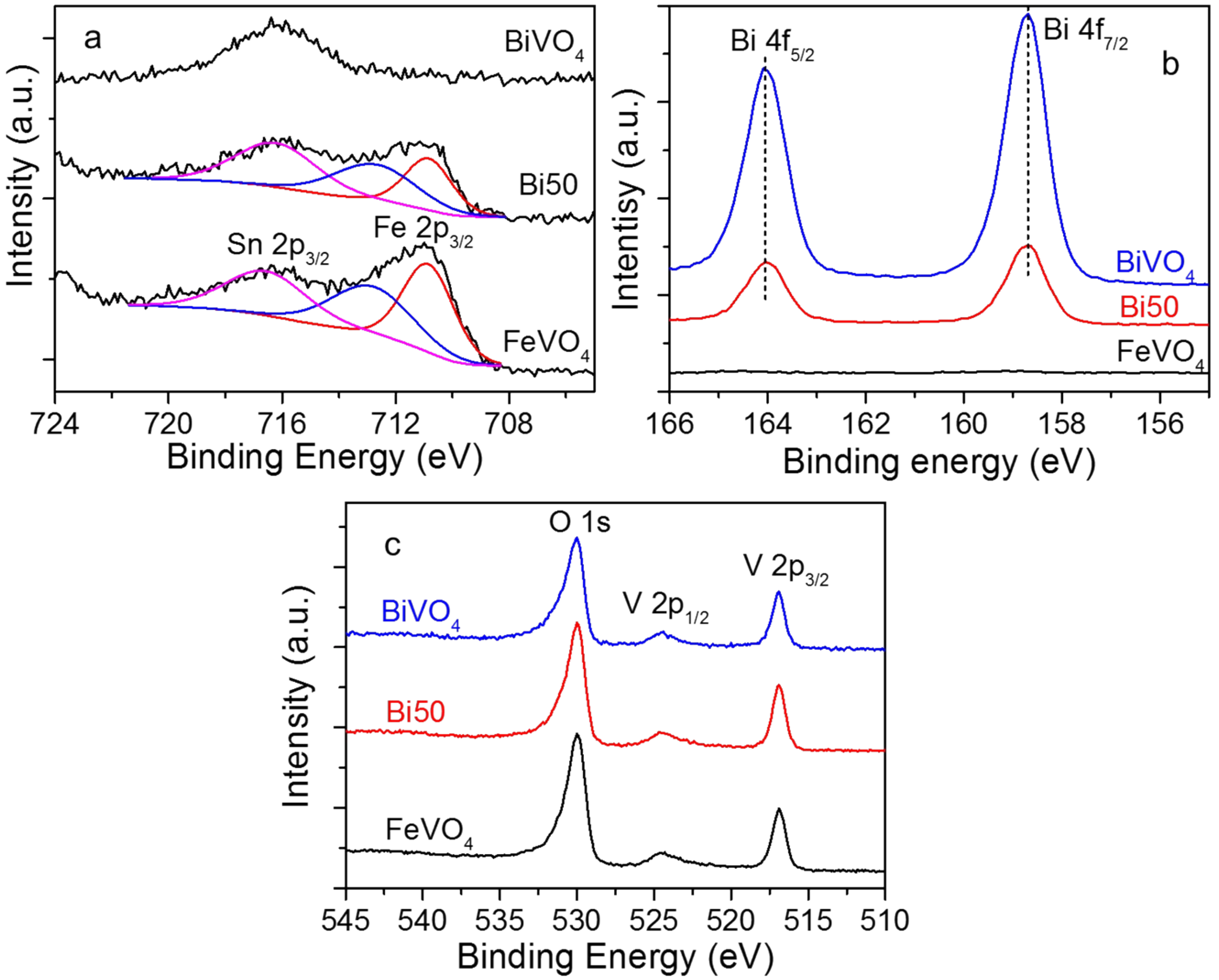

Figure S4 Fe 2p and Sn 3p (a), Bi 4f (b), V 2p and O 1s (c) XPS spectra for $FeVO_4$, Bi50 and $BiVO_4$ films.

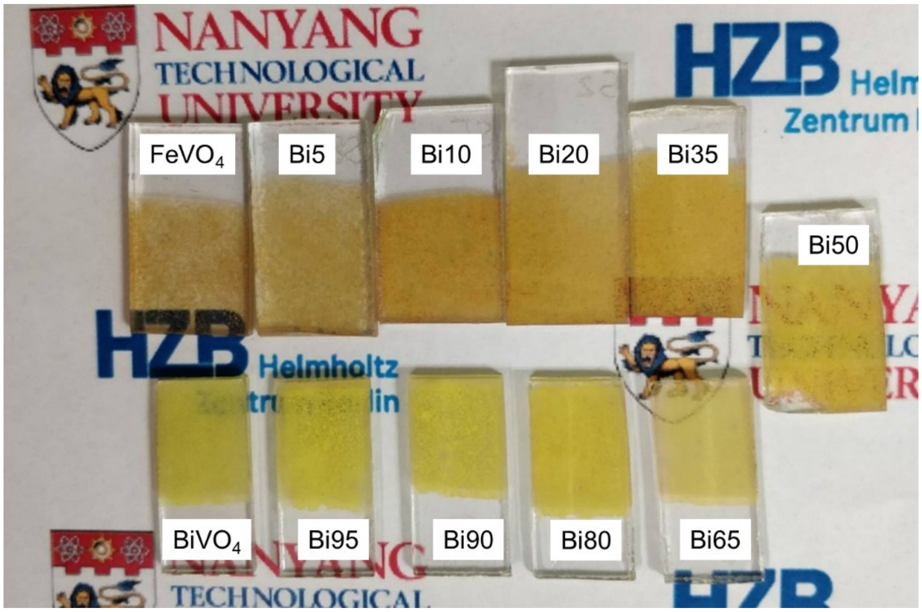

Figure S5 Photograph of films with various compositions, from $FeVO_4$ (upper left) to $BiVO_4$ (lower left).

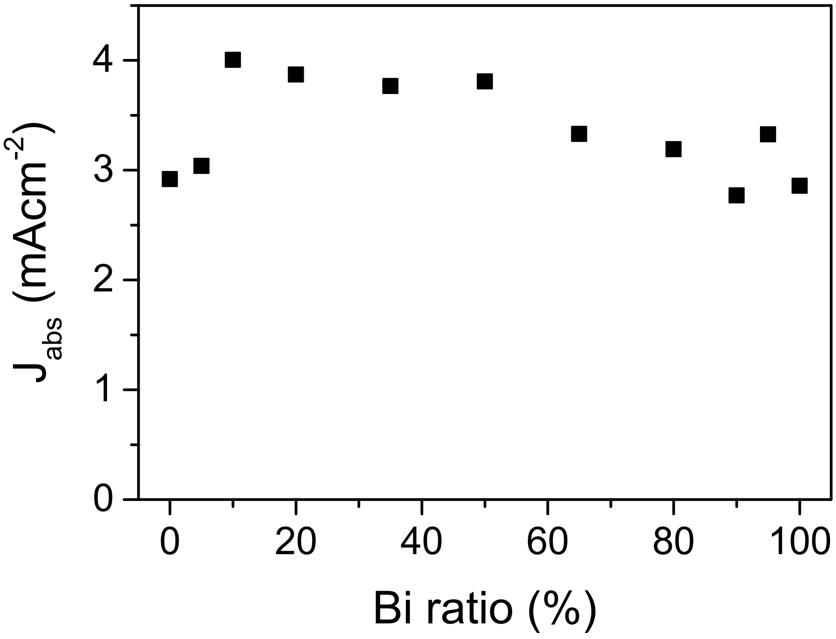

Figure S6 Calculated absorbed photocurrent density (J_{abs}) for the different films with varying Bi ratio.

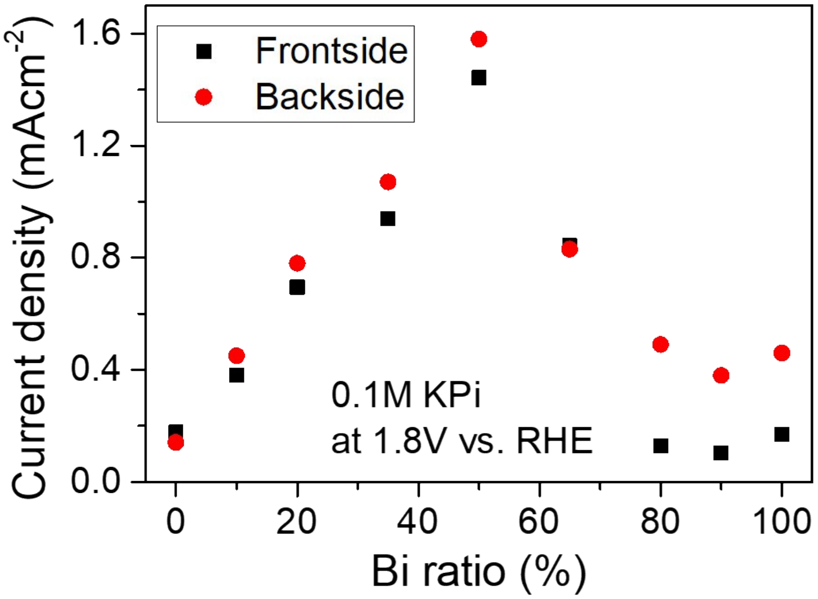

Figure S7 AM1.5 photocurrent density measured in 0.1 M KPi (pH = 7) under front and back illumination for films with different Bi ratio. The photocurrent values are taken at 1.8 V vs. RHE.

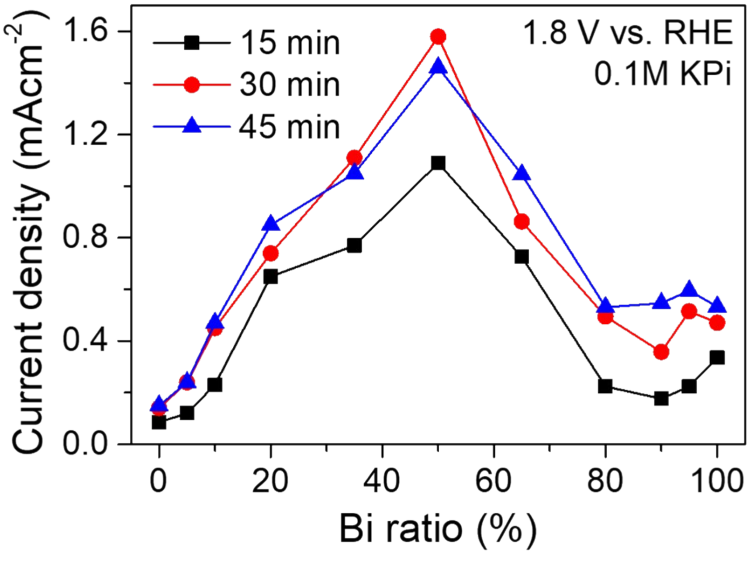

Figure S8 AM1.5 photocurrent-voltage curves of films with varying Bi ratio, deposited with different electrospinning time. The photocurrents were measured at 1.8 V vs. RHE in 0.1 M KPi under backside AM1.5 illumination.

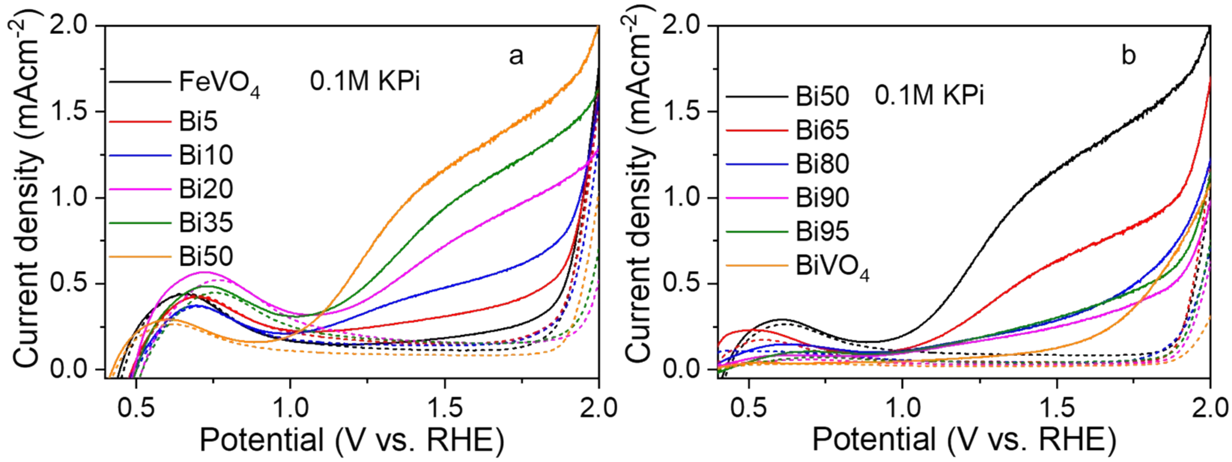

Figure S9 Original photocurrent curves for all compositions. Dark currents are indicated as dash lines while light currents are in solid lines.

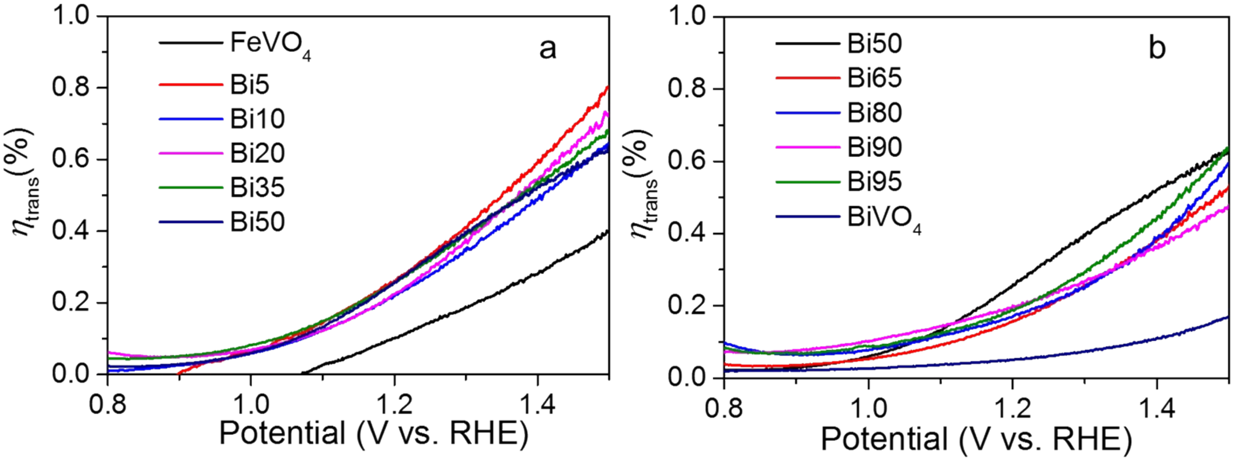

Figure S10 Charge transfer efficiency (η_{trans}) of all compositions as a function of applied potentials.

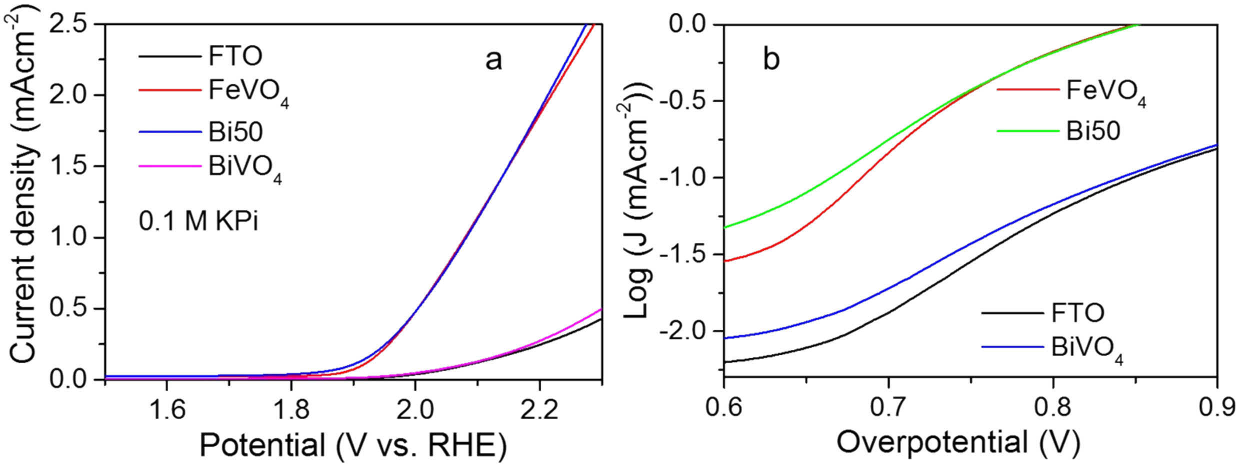

Figure S11 (a) Comparison of dark water oxidation activity of $BiVO_4$, $FeVO_4$ and Bi50 mixture film. FTO is also presented for reference. (b) The obtained Tafel plots from the dark J-V curves in (a).

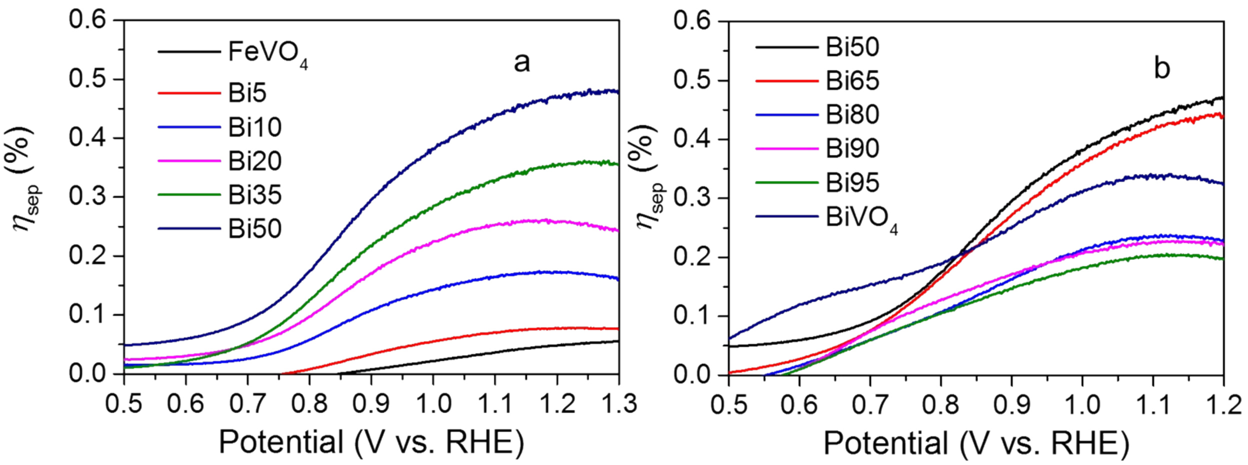

Figure S12 Charge carrier separation efficiency (η_{sep}) of all compositions as a function of applied potentials.

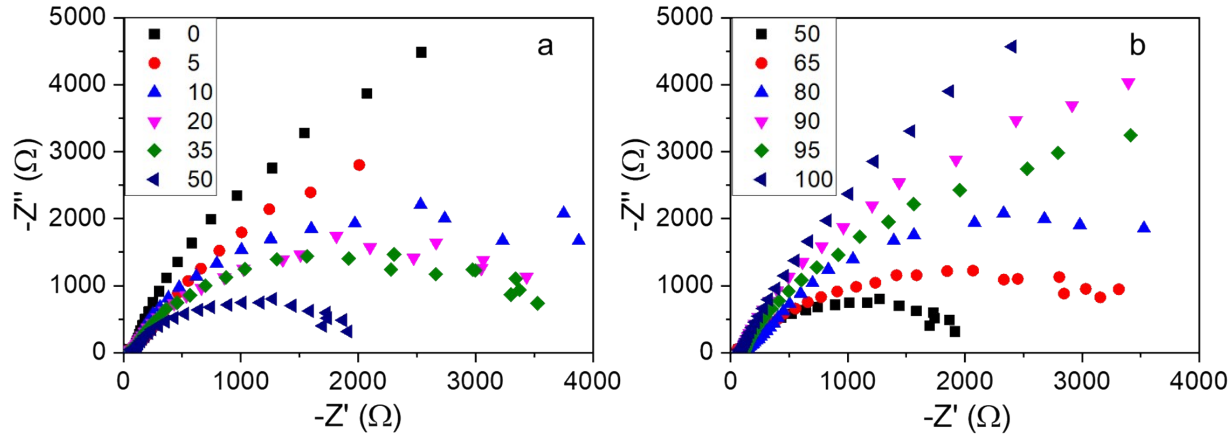

Figure S13 Nyquist plots for all composition films under AM1.5 illumination with an applied potential 1.23 V vs. RHE in 0.1M KPi.

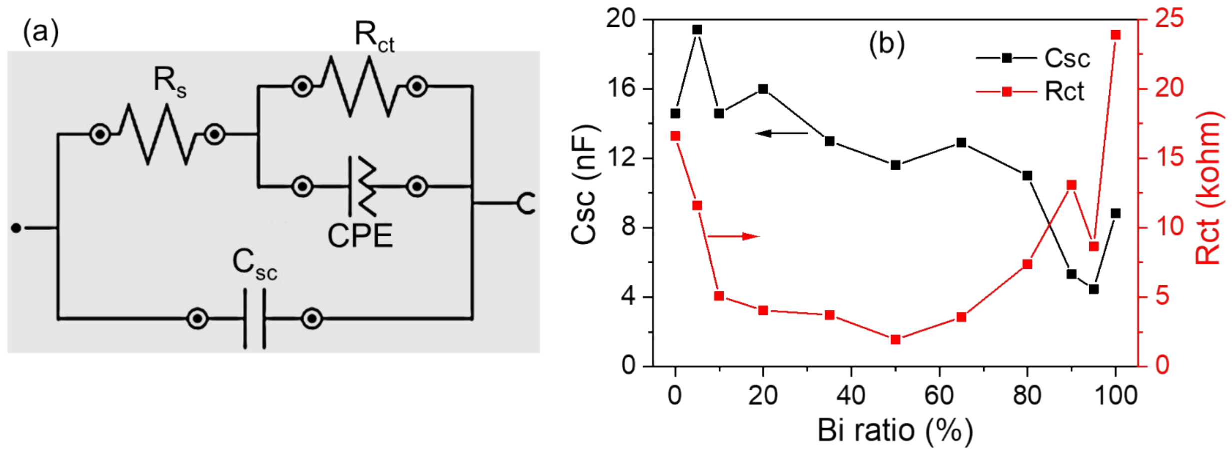

Figure S14 (a) Equivalent circuit for fitting Nyquist plots in **Figure S13**. (b) Trend of fitted R_{ct} and C_{sc} changing with Bi ratio. The R_s and Y_0 of the CPE are relatively constant for all samples and show no dependencies on the Bi ratio.

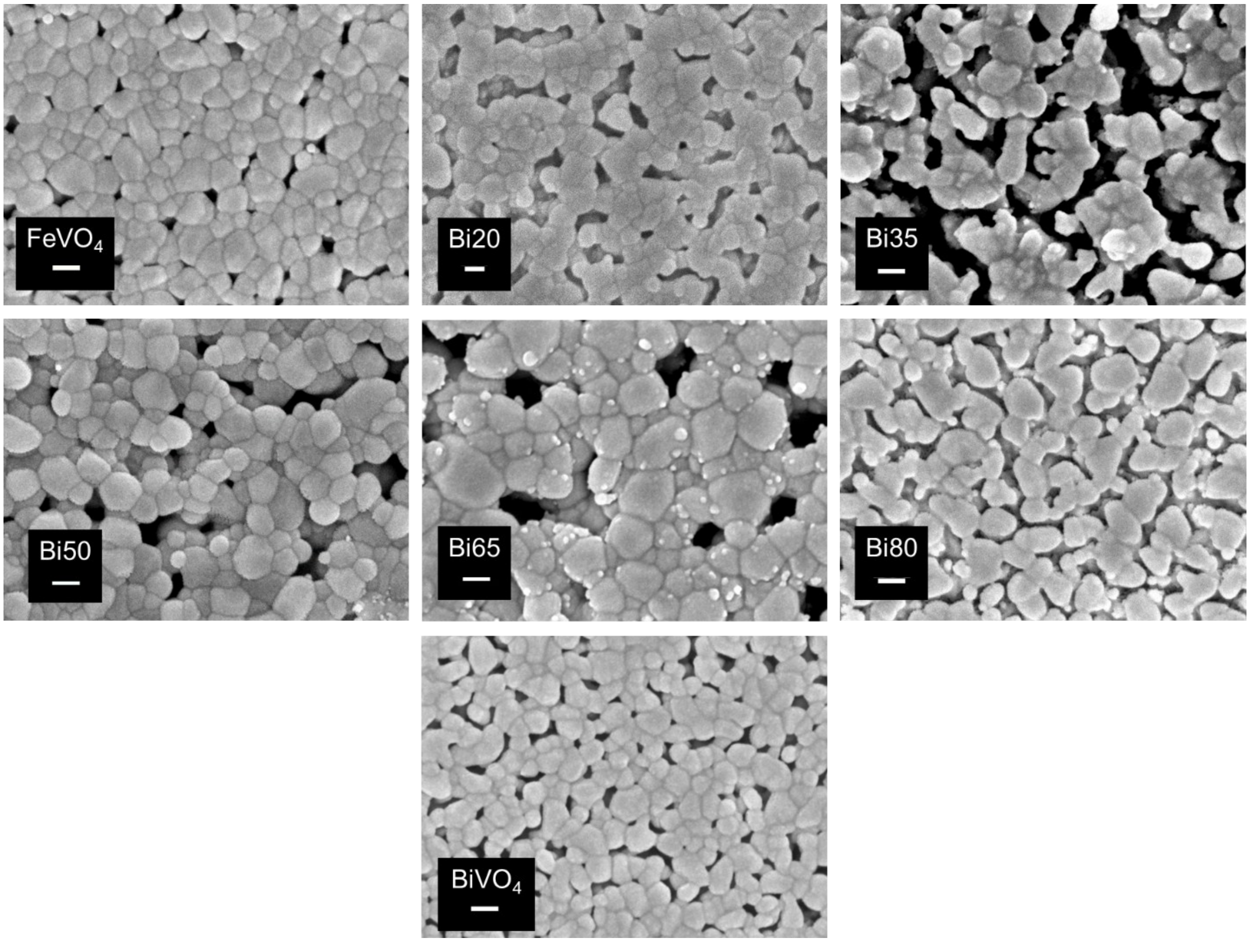

Figure S15 SEM images showing the surface morphology of the mixed vanadate films with different compositions. The scale bar indicated in each image represents 100 nm.

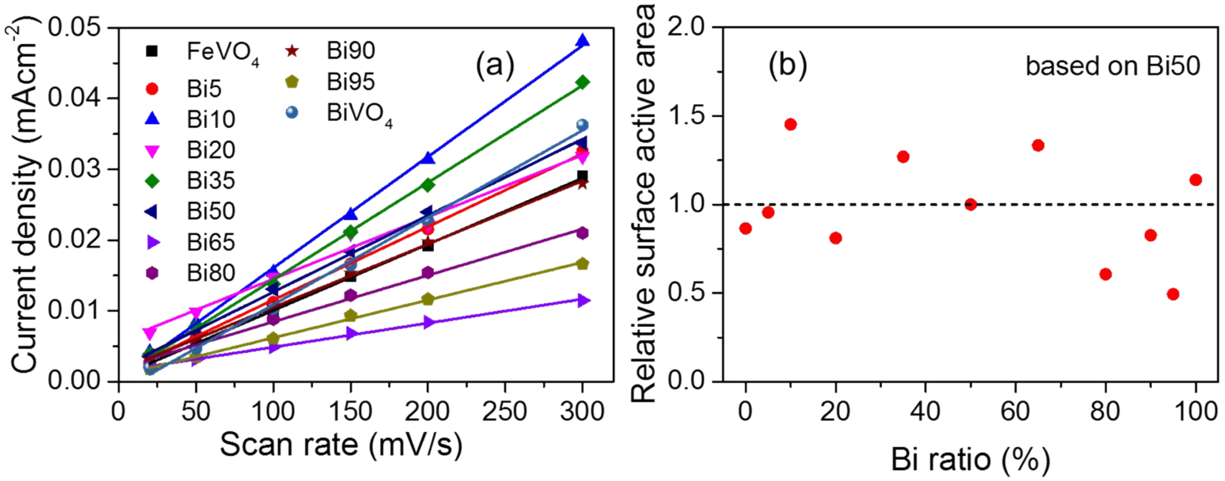

Figure S16 (a) Capacitive current as a function of scan rate for different compositions. (b) Calculated relative surface area normalized by Bi50 film, as obtained from the relative slope of the capacitive current.

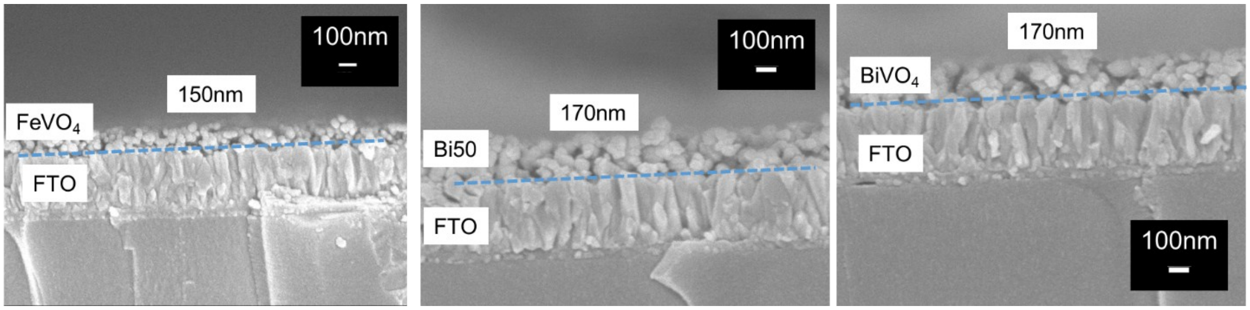

Figure S17 Cross-section view images for the 30 min electrospun $FeVO_4$, Bi50 and $BiVO_4$ films.

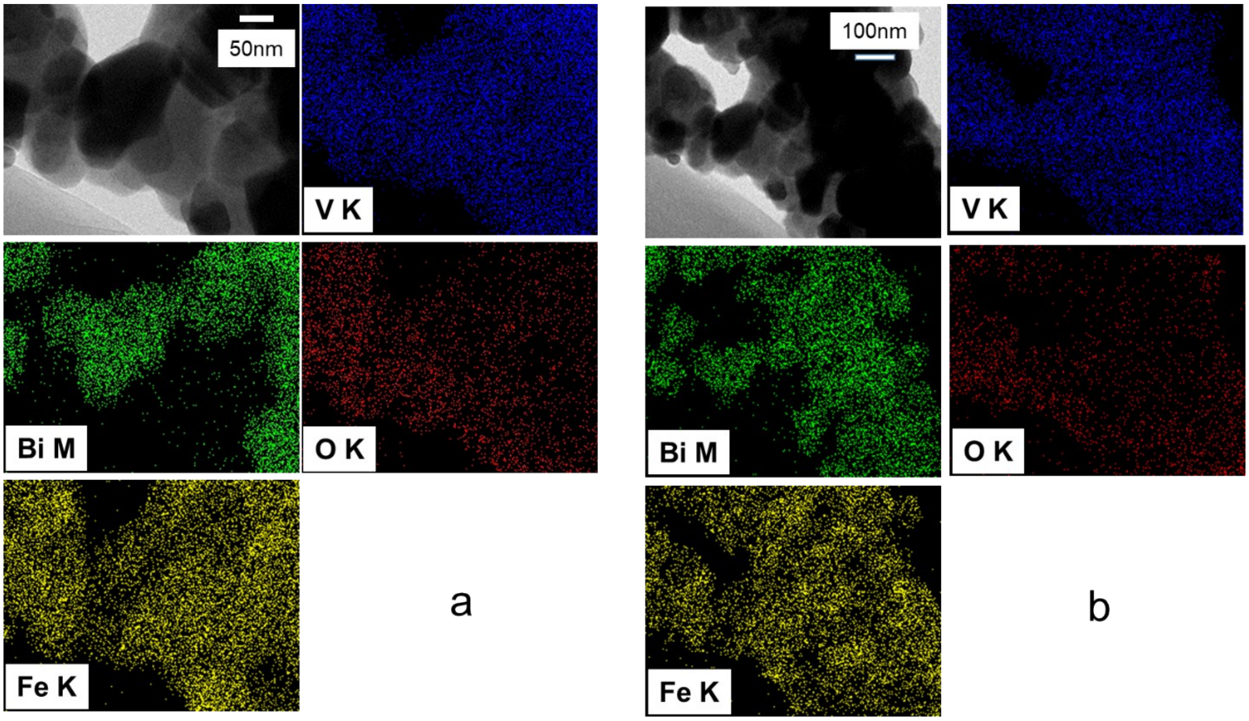

Figure S18 EDAX elemental mapping of Bi50 at two different locations (Figure 4c and d). Blue color represents V, green for Bi, red for O, and yellow for Fe.

Table S2 Atomic percent calculated from XPS peaks.

	Atomic percent (%)				
Sample	Bi	Fe	V	O	Fe/Bi
$FeVO_4$	0	13.2	10.3	76.5	-
Bi50	4.9	10.8	12.0	72.2	2.2
$BiVO_4$	18.98	0	10.4	70.6	0

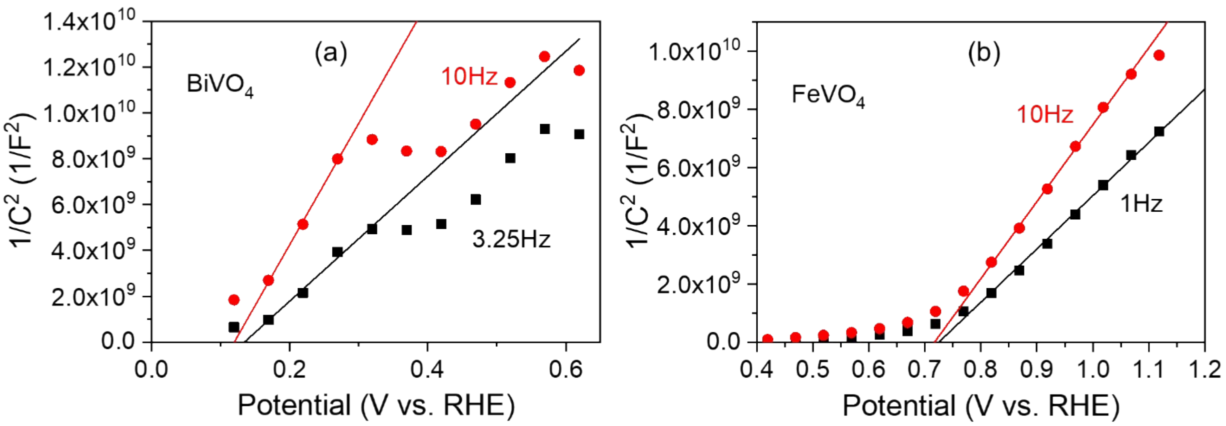

Figure S19 Mott-Schottky plots of BiVO$_4$ and FeVO$_4$ measured in 0.1M KPi. The low frequency was employed to obtain a good signal due to nanoporous structure.

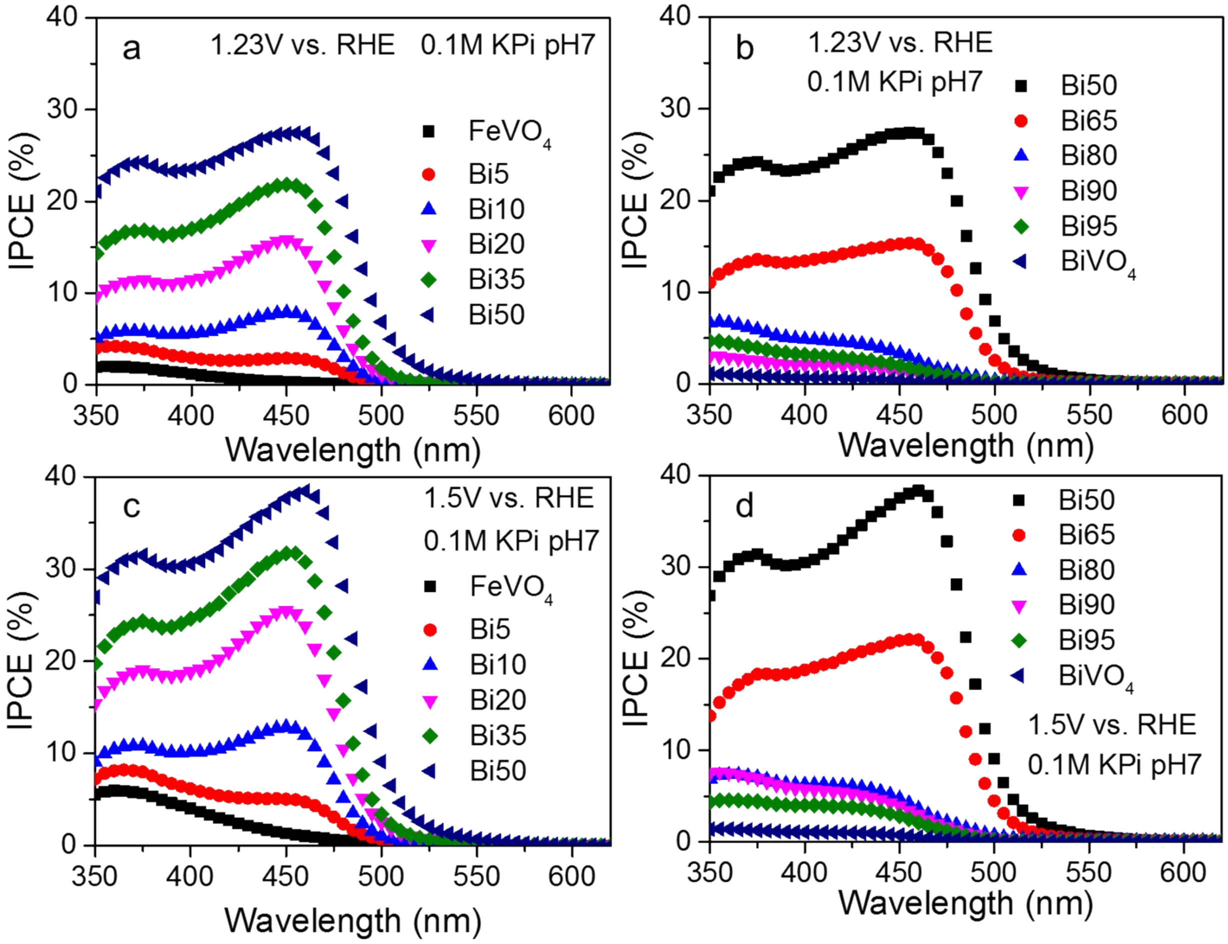

Figure S20 IPCE of all films measured in 0.1 M KPi at 1.23 V vs. RHE (a, b) and 1.5 V vs. RHE (c, d) respectively.

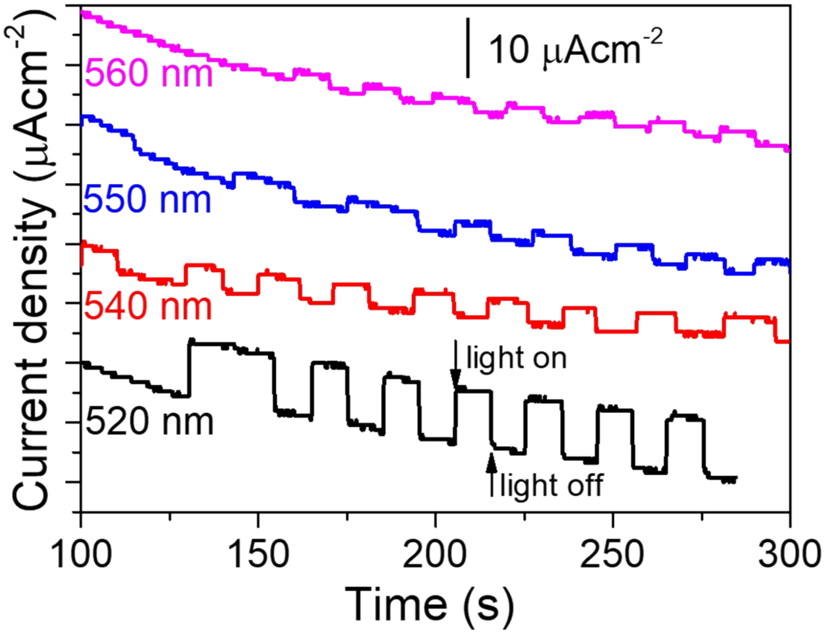

Figure S21 Current density of Bi50 under single wavelength illumination with applied potential 1.5 V vs. RHE in 0.1 M KPi + 0.5 M Na_2SO_3. The photo response under chopped illumination can be reflected in the current density change.

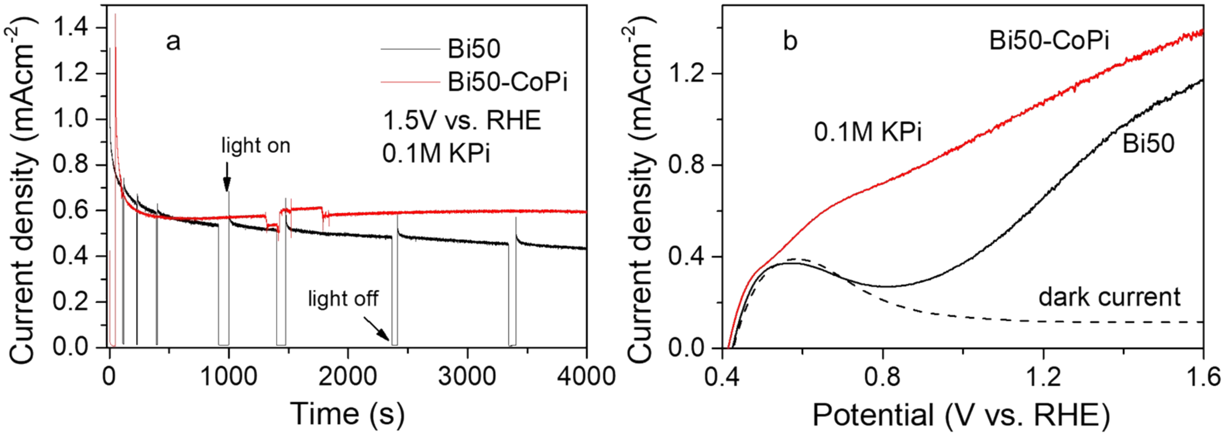

Figure S22 (a) Chronoamperometry measurement for Bi50 and CoPi deposited Bi50. The measurement was performed in 0.1 M KPi (pH=7) under illumination at a bias potential of 1.5 V vs. RHE. (b) AM1.5 photocurrent-voltage curves of Bi50 sample before and after CoPi deposition.

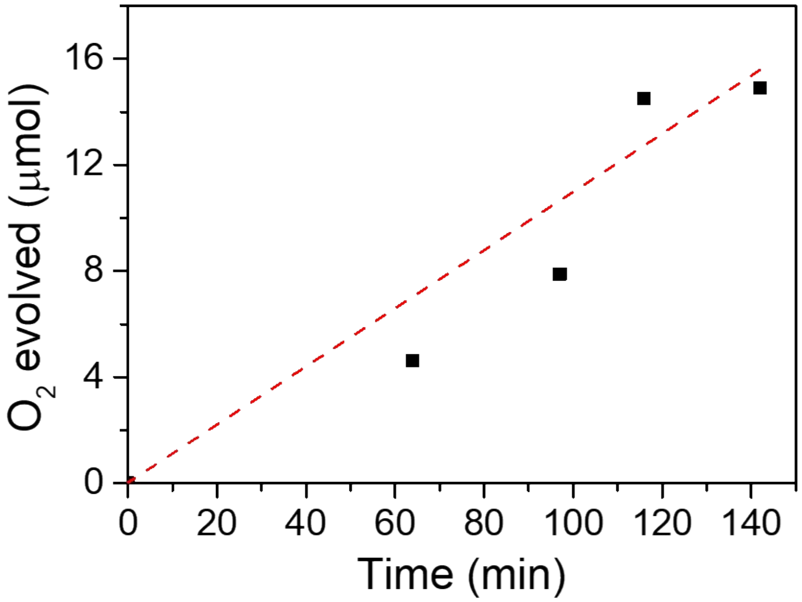

Figure S23 O_2 evolved from CoPi treated Bi50 film under AM1.5 illumination at 1.5 V vs. RHE. The red dash line indicates the theoretical amount of O_2 based on the charge from the current-time curve. Faradaic efficiency is then calculated to be ~88% by dividing the measured O_2 amount by the theoretical one.

References

1. F. F. Abdi, N. Firet and R. van de Krol, *ChemCatChem*, 2013, **5**, 490-496.
2. P. M. Rao, L. Cai, C. Liu, I. S. Cho, C. H. Lee, J. M. Weisse, P. Yang and X. Zheng, *Nano Letters*, 2014, **14**, 1099-1105.
3. J. Kibsgaard and T. F. Jaramillo, *Angewandte Chemie International Edition*, 2014, **53**, 14433-14437.
4. B. K. Kang, G. S. Han, J. H. Baek, D. G. Lee, Y. H. Song, S. B. Kwon, I. S. Cho, H. S. Jung and D. H. Yoon, *Advanced Materials Interfaces*, 2017, **4**, 1700323.